EAM
Environmental and Materials Journal
EAM 4(1): 17–35
ISSN 3025-0277

Institute for Advanced Science, Social and Sustainable Future
MORALITY BEFORE KNOWLEDGE

Non-linear soil chemical recovery toward a novel ecosystem in post-bauxite mining soils of tropical

Sulakhudin[1,*]

[1] *Department of Soil Science, Faculty of Agriculture, Universitas Tanjungpura, Pontianak, West Kalimantan 78124, Indonesia.*

*Correspondence: sulakhudin@faperta.untan.ac.id

Received Date: March 4, 2026 Revised Date: April 11, 2026 Accepted Date: April 20, 2026

ABSTRACT

Background: Reclaiming post-bauxite mining landscapes poses complex challenges owing to severe topsoil loss and drastic chemical alteration, yet phase-specific soil recovery trajectories in tropical Southeast Asia remain poorly characterized. This study evaluates the temporal dynamics of nine chemical properties across a post-bauxite reclamation chronosequence at PT XYZ, West Kalimantan, Indonesia. **Methods:** Soil samples were collected from eight sites, one natural forest control and seven reclaimed plots revegetated between 2014 and 2020 with three replicates per site, yielding 24 composite samples. Parameters encompassed pH, organic carbon, total nitrogen, available phosphorus, exchangeable cations, cation exchange capacity, base saturation, and exchangeable iron. Analyses included Pearson correlation, Principal Component Analysis, and K-means clustering validated by Silhouette analysis. **Findings:** Recovery proceeded through three non-linear phases: destabilization (5–7 years), transition (8–9 years), and initial stabilization (10–11 years). Soil pH showed the strongest recovery, with a mean recovery index of 109%, consistently surpassing the forest baseline. Iron exhibited the most critical deficit, averaging 19.9% recovery with a nadir of 2.0% at year seven, a micronutrient bottleneck not previously documented in tropical bauxite systems. Organic carbon and total nitrogen retained persistent deficits of 44.7% and 35.0%, respectively. The C–Fe coupling ($r = 0.784$) confirmed that iron mobilization is organically mediated, while PCA indicated that stabilization-phase soils occupy a distinct geochemical equilibrium separated from the forest reference. **Conclusions:** Post-bauxite recovery stabilizes into a novel ecosystem state with permanent deficits in iron, carbon, and nitrogen. The transition window at 8–9 years represents the optimal period for organic amendments and chelated iron applications to redirect the trajectory toward functional productivity. **Novelty/Originality of this article:** Providing the first quantitative evidence that recovery follows a non-linear, phase-dependent pathway converging toward a novel ecosystem state rather than the pre-mining forest baseline.

KEYWORDS: bauxite; chronosequence; iron deficiency; novel ecosystem; soil recovery.

1. Introduction

Bauxite mining is a strategic sector in Indonesia, significantly contributing to foreign exchange and supporting the downstream alumina industry. Open-pit extraction, however, inflicts profound ecological damage on the mined landscape (Dibattista et al., 2023). The process typically strips up to two meters of vegetation, topsoil, and overburden, eliminating nearly all natural habitat and hydrological function from the affected area (Annandale et al., 2021). What remains is a structurally degraded surface characterized by severe compaction, negligible organic matter, and a drastic decline in natural fertility (Yadav et al., 2022; Tibbett, 2024). Despite ongoing reclamation efforts by operators such as PT XYZ in West Kalimantan, post-bauxite soils in the region remain locked in a state of extreme physicochemical degradation, often exhibiting pH below 5.0 with acute nutrient deficiency

Cite This Article:
Sulakhudin. (2026). Non-linear soil chemical recovery toward a novel ecosystem in post-bauxite mining soils of tropical West Kalimantan. *Environmental and Materials*, *4*(1), 17-35. https://doi.org/10.61511/eam.v4i1.2026.3613

and elevated aluminum toxicity that collectively suppress natural vegetation succession (Suswati & Denashurya, 2023; Wanda et al., 2026). Whether these degraded conditions represent a transient stage or a persistent ecological state remains an open empirical question requiring systematic examination of the soil's chemical trajectory over time (Ghisman et al., 2025).

Answering that question demands a clear understanding of how mining dismantles the soil's biochemical architecture. Topsoil removal eliminates the organic fraction that serves as the soil's biological engine: Cavalcante et al. (2023) documented losses exceeding 99% of total carbon, nitrogen, and microbial biomass through the destruction of organic matter occluded within stable aggregates. Site-specific evaluations at Indonesian bauxite mines corroborate this severity; residual soil organic matter routinely falls below 1%, while total nitrogen and available phosphorus decline by 75% and 15.7%, respectively (Sulakhudin et al., 2023; 2024b). Such depleted organic matter levels cripple the soil's cation exchange capacity (CEC), which in kaolinite-dominated tropical soils derives primarily from organic rather than mineral surfaces (Cavalcante et al., 2023; Martins et al., 2021). The collapse of CEC, in turn, accelerates base cation leaching under the region's intense rainfall regime, creating a self-reinforcing cycle of nutrient impoverishment that extends well beyond the initial physical disturbance.

Breaking this impoverishment cycle is the central objective of reclamation, and revegetation with nitrogen-fixing pioneer species is widely regarded as the primary restorative mechanism. The effectiveness of revegetation, however, cannot be assessed at a single point in time, as recovery trajectories in post-mining soils are inherently dynamic, frequently exhibiting non-linear patterns of improvement, stagnation, and even regression over multi-year timescales (Nyenda et al., 2021). The chronosequence approach — substituting space for time by comparing reclaimed sites of different ages has become the standard methodology for capturing these dynamics in restoration ecology (Long et al., 2024). Applying this approach to bauxite systems, Lewis & Rosales (2020) estimated that pH and soil organic matter recovery may require 10 to 15 years, while Bizuti et al. (2022) found that essential nutrients consistently remain below pre-mining baselines in short-term chronosequences despite superficial canopy improvements. Longer-term evidence reinforces this trajectory: Nyenda et al. (2021) tracked pedogenesis on mine tailings over 110 years and concluded that recovery is polycyclic, with alternating phases of progression and retrogression rather than monotonic convergence. These findings collectively demonstrate that multi-temporal, multi-parameter assessments are essential to detect the phase transitions that govern reclamation success.

Detecting such phase transitions, in turn, requires understanding how soil chemical properties interact as coupled systems rather than independent variables. Organic matter accumulation can simultaneously boost CEC and mitigate heavy metal toxicity (Charan et al., 2025), yet decomposition of early-stage organic matter in acidic post-bauxite soils simultaneously releases proton-donating organic acids that may re-acidify the substrate if not counterbalanced by external ameliorants (Prematuri et al., 2020). Iron dynamics introduce further complexity: bauxite mining paradoxically depletes plant-available iron by removing the organically chelated topsoil fraction while exposing an Fe-oxide-rich substratum that locks residual phosphorus into insoluble forms (Wu et al., 2021; Yang et al., 2024). This dual mechanism of simultaneous iron deficiency and phosphorus fixation through a single geochemical pathway illustrates why isolated parameter assessments fail to capture the systemic constraints operating in post-mining soils. Multivariate approaches such as Principal Component Analysis (PCA) are therefore essential for disentangling these interacting trajectories and identifying the latent dimensions along which recovery proceeds (Tang et al., 2025; Souza et al., 2025).

When multivariate analyses are applied to sufficiently long chronosequences, a recurrent finding emerges: reclaimed soils rarely return to their pre-mining baseline. Permanent alterations in mineralogy, organic matter stocks, and microbial community composition force the landscape toward what restoration ecologists term a "novel ecosystem", a self-organizing state functionally distinct from the original forest (Annandale et al., 2021; Fernandes et al., 2021). Bizuti et al. (2022) formalized this as a "recovery debt," noting that subsurface properties may require centuries to approximate reference conditions or may never converge at all. Tibbett (2024) argued that acknowledging ecosystem novelty redirects management goals from unrealistic baseline replication toward optimizing functional productivity within the new edaphic reality. For tropical bauxite regions in Southeast Asia, however, empirical data supporting this framework remain scarce: Erusani et al. (2025) identified West Kalimantan as a critically under-studied region in the global post-mining sustainability literature, and Wanda et al. (2026) called specifically for location-specific amelioration research in the Sanggau Regency bauxite belt. Crucially, no study has yet quantified the phase-specific iron collapse or applied multivariate chronosequence analysis to characterize novel ecosystem formation in this region.

In response to this knowledge gap, the present study investigates post-bauxite soil chemical trajectories at the PT XYZ reclamation concession in Sanggau Regency as a model system for the humid tropics. The working hypothesis posits that reclaimed soils do not follow a direct trajectory toward the pre-mining forest baseline; rather, specific chemical parameters stagnate or regress, driving the system toward a novel ecosystem state. Three specific objectives are pursued to characterize the non-linear dynamics of individual soil parameters relative to the natural forest reference across a 5–11-year chronosequence, to identify distinct recovery phases through multivariate clustering, and to pinpoint the optimal intervention window and formulate phase-specific management recommendations for tropical post-bauxite reclamation landscapes.

2. Methods

2.1 Study area and site description

The research was conducted at the post-bauxite mining reclamation site operated by PT Aneka Tambang Tbk Unit Bisnis Pertambangan Bauksit (PT XYZ) in Tayan Hilir Village, Sanggau Regency, West Kalimantan, Indonesia (405,000–406,000 mE; 9,992,000–9,993,500 mN, UTM Zone 49S, WGS 1984) (Fig. 1). The study area is situated within the equatorial humid tropics, receiving mean annual precipitation exceeding 3,500 mm with no distinct dry season and a mean annual temperature of approximately 27 °C (Sulakhudin et al., 2024a).

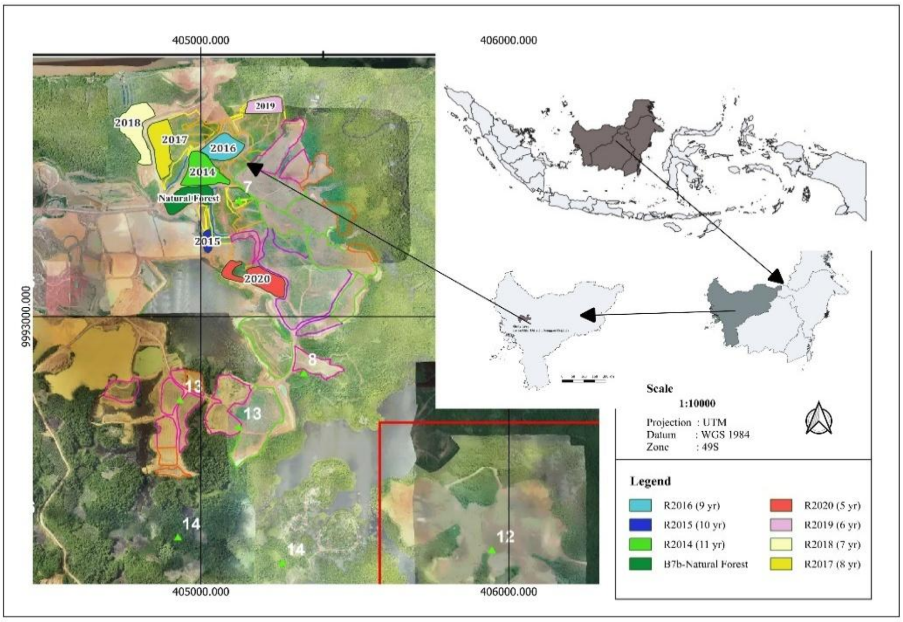

Fig. 1. Map of the study area at the PT XYZ post-bauxite mining reclamation site in West Kalimantan, Indonesia

Soils in the undisturbed portions of the concession are classified as Ultisols derived from lateritic parent material, characterized by a kaolinite-dominated clay fraction, low inherent cation exchange capacity, and naturally acidic reaction (pH 4.5–4.8). Prior to mining, the landscape supported lowland dipterocarp forest. Bauxite extraction at the site has followed a progressive sequence since 2014, with individual mining blocks cleared, extracted, and subsequently revegetated in successive annual cycles. Field sampling and laboratory observations were carried out between January and March 2025. All chemical analyses were performed at the Soil Chemistry and Fertility Laboratory, Faculty of Agriculture, Universitas Tanjungpura.

2.2 Experimental design and soil sampling

A chronosequence approach was adopted to evaluate the temporal dynamics of soil chemical properties across different reclamation ages. This space-for-time substitution method is widely employed in restoration ecology to reconstruct temporal trajectories from spatially distinct sites of known age (Nyenda et al., 2021; Tang et al., 2025). A total of 24 sampling points were purposively established across eight distinct strata: seven reclaimed areas revegetated between 2014 and 2020, corresponding to actual reclamation ages of 5 to 11 years at the time of sampling, and one unmined natural forest serving as the environmental baseline (control). To minimize confounding variables, site selection criteria ensured environmental uniformity across all plots, specifically requiring a slope gradient below 15%, identical pioneer vegetation cover, consistent historical ameliorant applications (dolomite liming and organic compost during land preparation), and matching geomorphological and lithological profiles between the reclaimed sites and the control forest. Representative field conditions across the chronosequence, including vegetation development, sampling procedures, and the lateritic substrate profile, are illustrated in Fig. 2.

Fig. 2. Field documentation at PT XYZ reclamation site (a) Acacia mangium revegetation plot (established 2018) with fern understory; (b) Soil core sampling using hand auger; (c) Lateritic soil profile from site B7a-R18 (depth 0–40 cm)

Soil sampling targeted the topsoil layer (0–20 cm depth) using a systematic composite sampling technique. At each of the 24 designated observation points, five sub-samples were collected: one from the central point and four additional samples situated approximately 25 m away in each cardinal direction. These sub-samples were thoroughly homogenized in the field. Approximately 1 kg of the well-mixed composite soil was retained, stored in sterile polyethylene bags, and transported to the laboratory under ambient conditions. Prior to chemical analysis, all samples were air-dried at room temperature, gently crushed, and passed through a 2-mm stainless-steel sieve to remove coarse debris and root fragments.

Two inherent limitations of the sampling design merit acknowledgement. First, the use of three composite replicates per site, while standard practice in post-mining chronosequence studies (Nyenda et al., 2021; Bizuti et al., 2022), constrains the statistical power available for detecting within-site variability. Second, the chronosequence approach assumes that all plots shared identical pre-mining conditions and differ only in time since revegetation; in practice, residual spatial heterogeneity in parent material composition, micro-topographic position, and ameliorant application intensity may introduce inter-site variability that the space-for-time substitution cannot fully resolve. These limitations are discussed further in the context of the Results.

2.3 Laboratory analysis

The nine parameters selected for analysis collectively represent the primary functional dimensions of soil chemical recovery in post-bauxite tropical systems: acid-base buffering (pH), biological carbon and nitrogen pools (SOC, TN), nutrient availability (available P, exchangeable K, Ca, Mg, Na), exchange complex capacity (CEC, BS), and micronutrient status (exchangeable Fe). This parameter set captures the coupled geochemical processes, organic matter, CEC, base cation interactions, and the Fe–P antagonism, identified as the dominant constraints on post-mining soil recovery in the literature (Cavalcante et al., 2023; Yang et al., 2024). All parameters were analyzed using standardized pedological protocols as follows.

Soil pH (H_2O) was measured electrometrically in a 1:2.5 soil-to-water suspension. Soil organic carbon (SOC) was determined by the Walkley and Black wet oxidation method, and total nitrogen (TN) was quantified via the macro-Kjeldahl digestion and distillation procedure. Available phosphorus (P) was extracted using the Bray-I method and quantified by spectrophotometry. Exchangeable basic cations (K, Ca, Mg, Na) were extracted with 1 N ammonium acetate (NH_4OAc) buffered at pH 7.0 and measured by Atomic Absorption Spectrophotometry (AAS). Cation exchange capacity (CEC) was determined using the same NH_4OAc extraction at pH 7.0, and base saturation (BS) was calculated as the percentage of CEC occupied by the sum of exchangeable basic cations. Exchangeable iron (Fe) was extracted using a 25% HCl solution to assess micronutrient availability. All analyses were performed in triplicate to ensure analytical reproducibility.

2.4 Data processing and statistical analysis

Statistical evaluation was conducted in R software version 4.3.0, utilizing the stats, Rcmdr, FactoMineR, and factoextra packages. Data were first assessed for normality (Shapiro-Wilk test, $\alpha = 0.05$) and homogeneity of variances (Levene's test). Independent t-tests ($\alpha = 0.05$) were then applied to compare each chemical parameter between individual reclamation ages and the natural forest control. A Pearson correlation matrix was generated to identify the strength and direction of bivariate relationships among all soil variables.

To reduce dataset dimensionality and visualize multivariate recovery trajectories, Principal Component Analysis (PCA) was performed on the standardized (z-score transformed) dataset encompassing all measured chemical and textural parameters. The first two principal components were retained for subsequent analysis. K-means cluster analysis was then applied to the PC1–PC2 coordinate space to classify the sampling sites into distinct recovery phases. The optimal number of clusters ($k = 3$) was determined by evaluating silhouette width scores across $k = 2$ to $k = 6$, with $k = 3$ yielding the highest mean silhouette coefficient, indicating the most internally cohesive and externally separated grouping. The extent of chemical recovery for each parameter at each reclamation age was quantified using the Recovery Index (RI):

$$RI\ (\%) = \frac{V_{reclaimed}}{V_{baseline}}\ x\ 100 \qquad \text{(Eq. 1)}$$

where V_reclaimed is the mean parameter value at a given reclamation site and V_baseline is the corresponding mean from the natural forest control. An RI of 100% indicates full recovery, values below 100% denote a persistent deficit, and values exceeding 100% indicate that the parameter has surpassed its pre-mining reference level. Mean deficits were subsequently calculated as gap indices (100% − mean RI) to quantify the overall recovery distance for each parameter.

3. Results and Discussion

Nine soil chemical parameters were measured across a post-bauxite mining chronosequence spanning reclamation ages from 5 to 11 years, with an adjacent undisturbed natural forest serving as the pre-mining reference baseline (Table 1). Soil pH ranged from 4.81 to 5.33 across all reclaimed plots, consistently exceeding the naturally acidic forest value of 4.66, whereas organic carbon and total nitrogen remained well below their respective baselines throughout. Available phosphorus exhibited the widest fluctuation, oscillating from 1.60 ppm at the 7-year site to 28.32 ppm at 9 years. Exchangeable iron declined most dramatically, falling from a forest baseline of 40.12 ppm to values rarely exceeding 15 ppm in any reclamation year. Cation exchange capacity fluctuated narrowly around the forest reference, while base saturation peaked at 26.27% in the youngest plot before converging toward the natural baseline of 11.85%. These data indicate that post-bauxite soils do not recover along a single linear trajectory; individual parameters follow distinct and often asynchronous pathways, the details of which are examined in the subsections that follow.

Table 1. Dynamics of key soil chemical properties across the post-bauxite mining reclamation chronosequence

Reclamation age	pH (H2O)	SOC (%)	Total N (%)	C/N	Avail. P (ppm)	CEC (cmol /kg)	BS (%)	Fe (ppm)
Natural Forest	4.66±0.03	2.82±0.11	0.29±0.03	9.92±0.92	7.88±0.83	10.54±1.01	11.85±0.64	40.12±3.75
5 Years	5.33±0.06	1.21±0.25	0.16±0.01	7.52±1.78	5.56±2.71	9.05±2.73	26.27±7.69	5.39±2.82
6 Years	5.17±0.20	1.19±0.26	0.16±0.01	7.62±1.38	9.88±2.57	9.51±1.09	14.78±3.17	2.58±0.18
7 Years	5.12±0.07	0.81±0.11	0.11±0.03	8.00±0.75	1.60±0.40	7.96±1.60	15.15±2.61	0.79±0.40
8 Years	4.97±0.07	1.87±0.05	0.22±0.03	8.64±1.00	21.80±5.55	10.23±2.49	16.78±5.37	11.70±2.28
9 Years	4.81±0.01	2.03±0.04	0.23±0.02	8.86±0.82	28.32±6.37	9.47±0.91	13.00±2.11	12.29±0.47
10 Years	4.96±0.04	2.18±0.06	0.24±0.04	9.65±1.47	21.70±2.60	10.94±0.07	12.57±1.44	8.24±0.77
11 Years	5.27±0.24	1.63±0.17	0.20±0.02	8.50±1.30	7.08±2.14	8.15±1.30	22.60±2.79	15.02±1.59

Note: All samples were analyzed in March 2025 at the Soil Chemistry and Fertility Laboratory, Faculty of Agriculture, Universitas Tanjungpura. Reclamation ages correspond to time elapsed since initial revegetation (2014–2020) at the time of sampling. Natural Forest = undisturbed reference site (B7a-Ha). SE = standard error of the mean from three independent composite replicates per site

3.1 Temporal dynamics of soil pH and acidity buffering

Across the entire chronosequence, all reclaimed sites recorded pH values consistently above the natural forest baseline of 4.66 (Table 1). The youngest reclamation plot (5 years) registered the highest pH at 5.33, while values at the 9-year site declined to 4.81 before rising again to 5.27 at 11 years. Recovery index calculations confirmed that pH surpassed its pre-mining reference at every sampling point, ranging from 103% (9 years) to 114% (5 years) (Fig. 3). This pattern of above-baseline pH aligns with observations reported by Bizuti et al. (2022) in Atlantic Forest bauxite mines and by Brasil et al. (2025) in the eastern Amazon, where reclaimed surfaces maintained higher pH than adjacent reference forests.

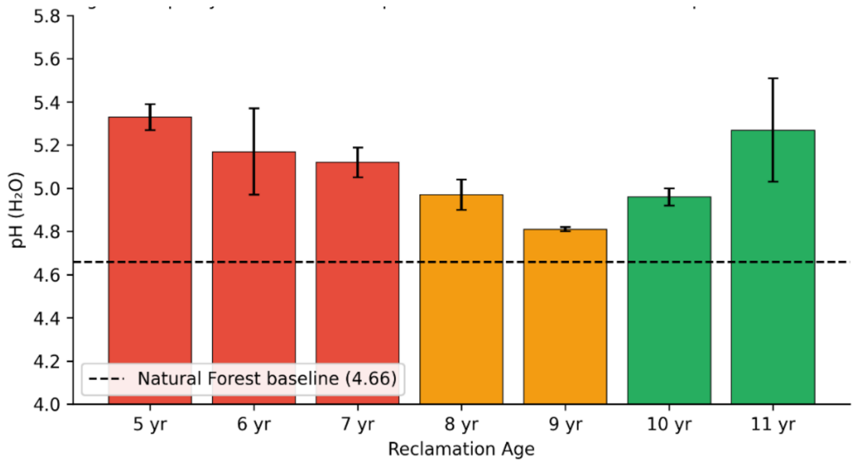

Fig. 3. Soil pH dynamics across the post-bauxite reclamation chronosequence. Dashed line indicates the natural forest baseline (pH 4.66). Colors denote recovery phases: red = destabilization (5–7 yr), yellow = transition (8–9 yr), green = stabilization (10–11 yr). Error bars represent ± SE (n = 3)

The elevated pH in younger plots reflects the residual alkalinity introduced during land preparation. Standard reclamation protocols at the study site include dolomite liming and organic compost incorporation prior to planting, both of which supply exchangeable Ca^{2+} and Mg^{2+} that displace acidic cations from exchange sites. Sulakhudin et al. (2024b) demonstrated that a single red mud application at a 1:250 soil ratio raised post-bauxite soil pH from 4.54 to 6.25 under field conditions in the same region, confirming the potency of alkaline ameliorants in these highly weathered substrates. The gradual pH decline observed between years 5 and 9 signals the progressive exhaustion of this initial buffering pool. As ameliorant-derived bases leach downward under the intense tropical rainfall regime exceeding 3,500 mm year^{-1} (Sulakhudin et al., 2024a), the soil increasingly reverts toward its naturally acidic equilibrium governed by aluminum hydrolysis and organic acid release (Daba, 2024).

A secondary pH rise at the 10–11-year sites introduces an ecologically meaningful inflection. The maturing Acacia canopy generates substantial leaf litter, and base cation cycling through plant uptake and litter decomposition partially replenishes the exchange complex (Bateman et al., 2021). Prematuri et al. (2020) cautioned, however, that decomposition of early-stage organic matter simultaneously releases proton-donating organic acids. Whether the system sustains its acid-neutralizing trajectory therefore depends on the balance between base cation inputs from vegetation cycling and proton generation from organic matter turnover. If external ameliorant applications cease entirely, models from analogous tropical systems suggest that this equilibrium may destabilize within one to two decades (Tsapko et al., 2023), potentially compromising the establishment of non-pioneer successional species. The close coupling between pH and nutrient retention capacity raises a broader concern: any erosion of the buffering system directly constrains the soil's capacity to accumulate organic carbon and nitrogen, the two parameters examined in the following sections.

3.2 Organic carbon depletion and the pace of soil biological recovery

Soil organic carbon concentrations in the natural forest averaged 2.82%, representing the functional baseline against which all reclaimed sites were compared (Table 1). Across the chronosequence, SOC exhibited a distinct non-linear trajectory. The youngest sites (5–6 years) retained only 1.21% and 1.19%, respectively, indicating severe depletion. A conspicuous minimum appeared at the 7-year site (0.81%), after which SOC rose progressively through the transition and stabilization phases, reaching 2.18% at 10 years before declining again to 1.63% at 11 years. Even at the point of maximum recovery (10 years), the system retained a 22.7% deficit relative to the forest reference; when averaged across the entire chronosequence, this gap widened to 44.7% (Fig. 4).

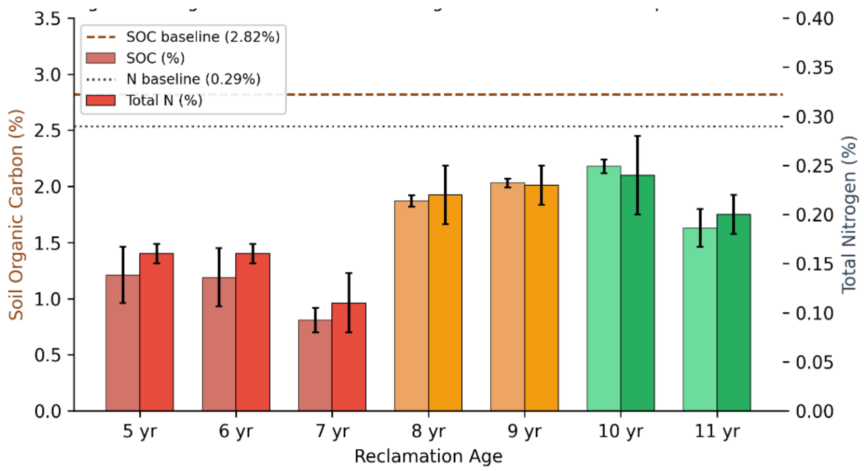

Fig. 4. Soil organic carbon and total nitrogen across the chronosequence. Dashed and dotted lines indicate respective natural forest baselines. Error bars represent ± SE (n = 3)

Such carbon loss traces directly to the mechanical stripping of biologically active topsoil during bauxite extraction. Cavalcante et al. (2023) documented that mining operations can eliminate up to 99% of total carbon, nitrogen, and microbial biomass by destroying organic fractions occluded within stable soil aggregates. At the study site, Sulakhudin et al. (2023) previously reported that post-mining SOC levels drop below 1%, consistent with the 7-year site recorded here. The gradual accumulation observed from 8 to 10 years reflects the onset of canopy closure in Acacia stands, which deposits increasing quantities of fine litter onto the soil surface. Souza et al. (2025) observed a comparable SOC increase between 4- and 9-year natural regeneration plots in Amazonian bauxite mines and attributed it primarily to root exudate contributions in the topsoil horizon.

The decline from 2.18% at 10 years to 1.63% at 11 years warrants careful interpretation. Rather than representing true carbon loss, this drop likely reflects spatial heterogeneity inherent to the chronosequence approach, where each age class occupies a different physical plot (Hermansyah et al., 2021). Spletozer et al. (2024) encountered analogous site-to-site variability in southeastern Brazilian bauxite mines and stressed that space-for-time substitutions assume identical starting conditions — an assumption rarely satisfied in heterogeneous mining landscapes. Regardless of the cause, organic carbon rebuilding in post-bauxite soils proceeds at a rate insufficient to reconstitute the pre-mining pool within a single decade. Bizuti et al. (2022) conceptualized this persistent shortfall as a "recovery debt," a cumulative biological deficit that accrues when destruction occurs rapidly but repair operates on ecological timescales spanning decades to centuries. The most immediate consequence of this carbon deficit is its downstream effect on nitrogen cycling, given the tight biogeochemical coupling between the two elements.

3.3 Nitrogen cycling constraints and C–N coupling

Total nitrogen followed a trajectory closely parallel to SOC, declining from a baseline of

0.29% to 0.16% in the youngest plots and reaching its lowest value of 0.11% at the 7-year site (Table 1). The Pearson correlation between SOC and total N was strongly positive (r = 0.812), confirming that carbon and nitrogen dynamics in these soils are tightly coupled through shared organic matter pools. C/N ratios across the chronosequence ranged from 7.52 to 9.65, consistently below the forest reference of 9.92. Narrower C/N ratios in the younger reclamation plots indicate a relative enrichment of nitrogen in the residual organic fraction, attributable to the nitrogen-fixing capacity of the Acacia pioneer vegetation combined with the preferential mineralization of labile carbon compounds under tropical temperatures (Ouyang et al., 2023).

Nitrogen recovery mirrored the same non-linear curve as SOC, improving from 55% of baseline at 5–6 years to 83% at 10 years before declining to 69% at 11 years. Despite this partial improvement, the chronosequence mean revealed a persistent 35.0% nitrogen deficit. Hartati et al. (2025) identified organic matter as the single most influential variable governing nitrogen availability in the topsoil of post-mining sites, a finding that resonates with the C–N coupling observed here. The strong correlation also implies that any strategy targeting nitrogen replenishment must simultaneously address carbon accumulation — mineral nitrogen fertilizers alone would provide only a transient pulse rather than the stable organic reservoirs necessary for sustained nitrogen mineralization.

From a functional standpoint, the nitrogen deficit may constrain the developing ecosystem's trophic chain. Insufficient nitrogen supply may limit photosynthetic capacity and slow canopy expansion, consequently reducing litter return to the soil and reinforcing the recovery debt (Enescu et al., 2025). Breaking this cycle requires exogenous organic inputs of sufficient magnitude to overcome the mineralization-dominated steady state. Larney & Angers (2012) recommended applications of 10–20 Mg ha^{-1} of composted manure to accelerate organic carbon and nitrogen accumulation in degraded lands, a dosage supported by field trials in Indonesian bauxite mines using combined red mud and cattle manure amendments (Wanda et al., 2026). Beyond nitrogen accumulation, the availability of phosphorus introduces additional complexity through its antagonistic interaction with iron oxides.

Table 2. Carbon-nitrogen coupling indicators across the post-bauxite mining chronosequence

Age	SOC (%)	N (%)	C/N	SOC RI (%)	N RI (%)	Coupling
Forest	2.82±0.11	0.29±0.03	9.92	100.0	100.0	Baseline
5 yr	1.21±0.25	0.16±0.01	7.52	42.9	55.2	N enriched
6 yr	1.19±0.26	0.16±0.01	7.62	42.2	55.2	N enriched
7 yr	0.81±0.11	0.11±0.03	8.00	28.7	37.9	N enriched
8 yr	1.87±0.05	0.22±0.03	8.64	66.3	75.9	Converging
9 yr	2.03±0.04	0.23±0.02	8.86	72.0	79.3	Converging
10 yr	2.18±0.06	0.24±0.04	9.65	77.3	82.8	Near-baseline
11 yr	1.63±0.17	0.20±0.02	8.50	57.8	69.0	Converging

Note: SOC RI and N RI = Recovery Index calculated as (V_reclaimed / V_baseline) × 100 relative to the natural forest reference. Coupling status: "N enriched" = N RI exceeds SOC RI by >10 percentage points, reflecting preferential nitrogen retention via Acacia fixation; "Converging" = gap narrowing to <10 points; "Near-baseline" = both indices ≥75% with C/N approaching the forest reference. Pearson r = 0.990 (site means, n = 8)

3.4 Phosphorus availability and Fe–P antagonism

Available phosphorus displayed the most volatile pattern among all evaluated parameters (Table 1). From a baseline of 7.88 ppm, P dropped sharply to 1.60 ppm at the 7-year site, surged to 28.32 ppm at 9 years, and subsequently declined to 7.08 ppm at 11 years. This erratic fluctuation contrasts with the relatively smooth trajectories of pH and SOC, suggesting that phosphorus availability in these soils is governed by multiple competing mechanisms operating at different temporal scales (Fig. 5).

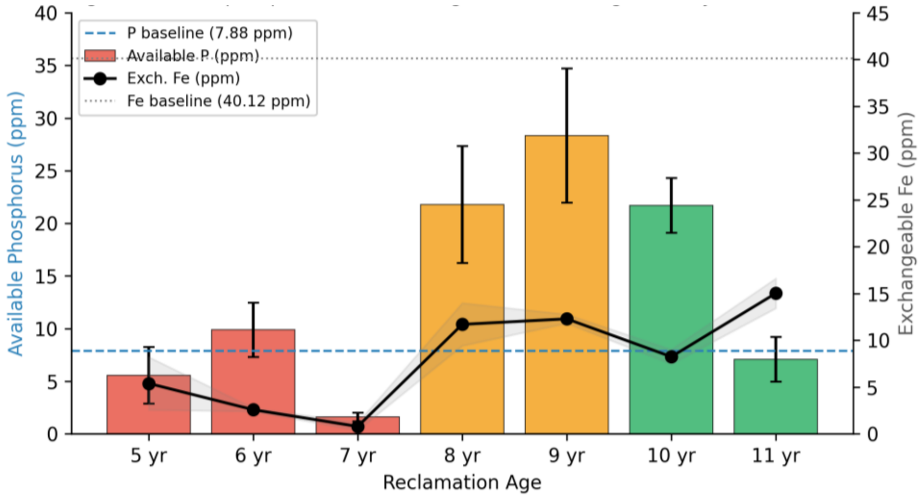

Fig. 5. Antagonistic dynamics of available phosphorus (bars, left axis) and exchangeable iron (line, right axis) across the chronosequence. Gray shading around the Fe line represents ± SE

Two principal processes explain the observed pattern. First, the extremely low P at the 7-year site coincides with the lowest SOC (0.81%) and Fe (0.79 ppm) values in the chronosequence. At such depleted organic matter levels, the soil lacks the organic ligands necessary to compete with mineral surfaces for phosphate ions, and iron and aluminum oxides in these lateritic substrates readily adsorb dissolved phosphate into forms inaccessible to plant roots (Wu et al., 2021; Yang et al., 2024). Second, the pronounced P spike at 8–9 years coincides with the transition phase, during which residual fertilizer P likely becomes mobilized as increasing organic acid concentrations from accumulating litter begin to solubilize previously fixed P pools. Cavalcante et al. (2023) identified available P as one of the most management-sensitive parameters in post-bauxite soils, responding sharply to combined organic and chemical fertilization. The subsequent P decline at 10–11 years may reflect plant uptake outpacing replenishment, or renewed fixation as litter-derived organic acids are consumed.

This phosphorus volatility carries practical significance for reclamation management. Targeted phosphate fertilization timed to the transition phase (8–9 years), when organic matter accumulation is actively solubilizing fixed pools, may capitalize on a naturally favorable geochemical window. Applying phosphate fertilizer during the destabilization phase (5–7 years), by contrast, risks reducing the efficiency of applied phosphate through Fe-oxide fixation. This antagonistic Fe–P dynamic connects directly to the broader pattern of cation exchange dynamics across the chronosequence.

3.5 Cation exchange dynamics, base saturation, and exchangeable bases

Cation exchange capacity values fluctuated between 7.96 and 10.94 cmol kg^{-1} across the chronosequence, bracketing the forest reference of 10.54 cmol kg^{-1} (Table 1, Fig. 6a). The 7-year site recorded the lowest CEC (7.96 cmol kg^{-1}), consistent with its simultaneously minimal SOC, confirming that organic matter is the primary contributor to the exchange complex in these predominantly kaolinitic, low-activity clay soils (Cavalcante et al., 2023). By the 10-year site, CEC recovered to 10.94 cmol kg^{-1}, marginally exceeding the baseline — as organic matter accumulation rebuilt the exchange surfaces. Martins et al. (2021) reported a comparable CEC trajectory in Amazonian bauxite Technosols, where constructed soil layers approached reference forest CEC values only after sufficient liming and organic amendment.

Base saturation, in contrast, exhibited a pattern distinctly decoupled from CEC. The forest baseline registered an exceptionally low BS of 11.85% (Fig. 6b), characteristic of the highly leached Ultisols of equatorial West Kalimantan. The youngest reclamation plot (5 years) showed a dramatically elevated BS of 26.27%, which then declined progressively to 12.57% at 10 years before rising again to 22.60% at 11 years. This initial inflation reflects ameliorant-derived base cation loading; dolomite and compost applications introduce Ca^{2+}, Mg^{2+}, K^{+}, and Na^{+} that temporarily saturate the exchange complex. As these bases leach under high rainfall, BS converges toward the naturally low equilibrium of the reference soil (Sulakhudin et al., 2024a). The strong positive correlation between pH and exchangeable K (r = 0.818) corroborates this interpretation: as base cations diminish, so does the soil's capacity to maintain the modestly elevated pH recorded in younger plots.

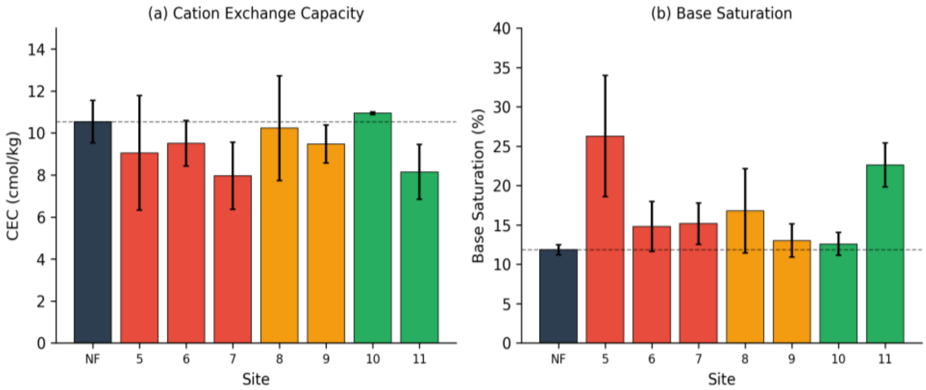

Fig. 6. (a) Cation exchange capacity and (b) base saturation dynamics across the chronosequence. NF = natural forest. Dashed lines indicate baseline values. Error bars represent ± SE (n = 3)

The pH–K correlation identifies potassium mobility as a practical indicator of leaching intensity in these reclaimed soils. Daba (2024) emphasized that in reconstructed mine soils where weatherable mineral reserves are negligible, external base cation inputs remain the only reliable buffering source, a dependence that extends to micronutrients, among which iron represents the most critically deficient element (Lilay et al., 2024).

3.6 Iron deficiency and micronutrient imbalance

Among all evaluated parameters, exchangeable iron exhibited the most severe and persistent deficit relative to the forest baseline (Table 1, Fig. 7). The natural forest maintained an average Fe concentration of 40.12 ppm, whereas reclaimed sites ranged from 0.79 ppm at 7 years to a maximum of only 15.02 ppm at 11 years. The destabilization phase (5–7 years) proved especially critical for iron availability, with three consecutive sites recording concentrations of 5.39, 2.58, and 0.79 ppm, collectively averaging only 7.3% of the baseline level. Even the best-performing reclamation site retained merely 37.4% of pre-mining Fe, and the chronosequence mean (8.54 ppm) represented an 80.1% deficit by far the largest gap recorded for any parameter.

This depletion appears counterintuitive in a landscape derived from bauxite ore, which is mineralogically dominated by iron and aluminum oxides. Stripping operations, however, selectively remove the biologically active topsoil horizon where plant-available Fe exists in organically chelated forms, predominantly as Fe^{2+}-humate and Fe^{3+}-fulvate complexes (Raj et al., 2020). The exposed lateritic substratum retains enormous quantities of total iron, but overwhelmingly in crystalline oxide phases (goethite, hematite) that resist dissolution under the mildly acidic pH conditions (4.8–5.3) prevailing across the chronosequence. Xie et al. (2025) demonstrated that iron-organic complexes are essential for both plant Fe uptake and soil aggregate stability, and that their absence forces iron into geochemically inert pools. The strong positive correlation between SOC and Fe (r = 0.784) observed here supports that mechanism: as organic carbon accumulates through the transition and stabilization phases, an increasing proportion of total iron is mobilized into exchangeable forms through organic complexation.

The functional consequences of this iron deficit extend beyond micronutrient nutrition alone. Fe-oxide surfaces exposed by mining actively fix available phosphorus into occluded forms, establishing the antagonistic Fe–P dynamic discussed in Section 3.4. Yang et al.

(2024) described this dual role of iron oxides as simultaneously constraining two essential nutrients through a single geochemical mechanism. Symptoms consistent with coupled Fe–P deficiency, including chlorosis and stunted growth in non-pioneer colonizers, have been reported in analogous post-bauxite systems (Gao et al., 2026). Correcting the iron deficit without exacerbating phosphorus fixation requires chelated Fe amendments, such as Fe-EDDHA or ferrous sulfate co-applied with organic matter to simultaneously supply chelating ligands. Sulakhudin et al. (2024b) showed that red mud, rich in reactive iron, can serve a dual function as both a pH ameliorant and an iron source when combined with organic supplements to prevent SOC depression. The convergence of all these individual parameter trajectories into a coherent spatial pattern is most clearly revealed through multivariate analysis.

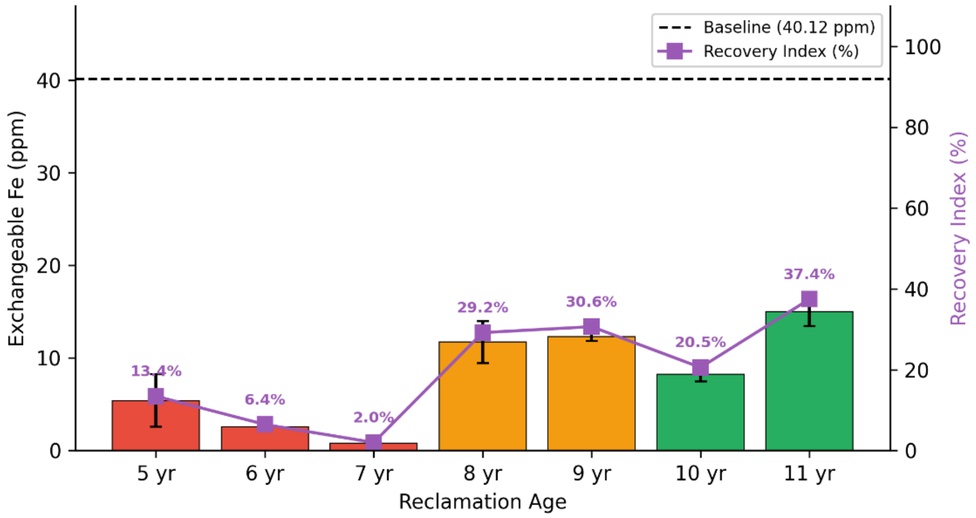

Fig. 7. Exchangeable iron depletion (bars, left axis) and Recovery Index (line with squares, right axis) across the chronosequence. Percentage labels indicate RI for each site. Dashed line = baseline (40.12 ppm)

3.7 Multivariate recovery trajectory and phase identification

Principal Component Analysis condensed the multidimensional dataset into two principal axes accounting for 61.2% of total variance (PC1 = 38.5%; PC2 = 22.7%) (Fig. 8). The PC1 axis separated sites along a gradient defined by pH, exchangeable bases (K, Ca, Mg, Na), and base saturation on the positive end, opposed by organic carbon, nitrogen, and exchangeable acidity on the negative end. PC2 captured variation driven by available phosphorus and CEC on the negative end versus sand content on the positive end. The natural forest samples clustered tightly in the negative PC1 / positive PC2 quadrant — characterized by high organic carbon, nitrogen, and iron but low pH and base saturation — consistent with the mature, highly weathered Ultisol profile expected under undisturbed tropical forest.

K-means clustering (k = 3), validated by Silhouette analysis, delineated three distinct recovery phases that did not follow a simple linear trajectory toward the forest reference. The destabilization phase (5–7 years; sites R20, R19, R18) occupied a wide, dispersed region in the positive PC1 / positive PC2 space, reflecting high internal variability and biogeochemical instability. These sites retained the chemical signature of initial ameliorant applications, elevated pH and base saturation, while simultaneously exhibiting severe organic carbon and iron depletion. Nyenda et al. (2021), using PCA on a 110-year gold tailings chronosequence, identified an analogous early-stage cluster characterized by extreme geochemical disequilibrium. The broad scatter of destabilization-phase points in the present study reinforces that interpretation: the soil system at 5–7 years has not yet converged toward a consistent geochemical trajectory.

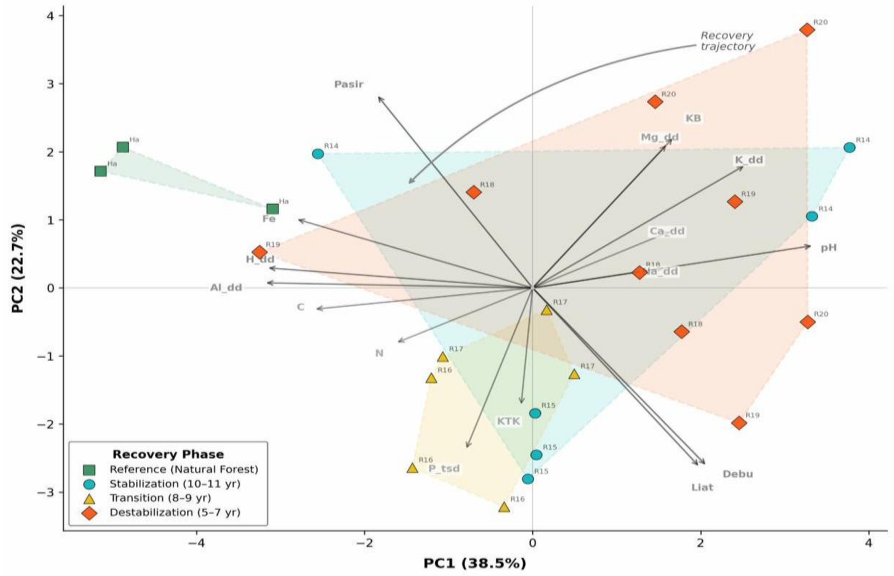

Fig. 8. PCA biplot of soil chemical properties across the post-bauxite mining chronosequence. Ellipses denote K-means clusters (k = 3): destabilization (5–7 yr), transition (8–9 yr), and stabilization (10–11 yr). NF = natural forest reference

The transition phase (8–9 years; sites R17, R16) shifted into the negative PC2 domain, driven by rapidly increasing available P and CEC as organic matter accumulation began restructuring the exchange complex. Tang et al. (2025) documented a comparable transition in Chinese coal mine chronosequences, where soil quality indices increased most steeply between years 5 and 8 before flattening in older plots. The 8–9-year window therefore represents the period of maximum biogeochemical flux and the optimal timing for intensive secondary interventions such as organic amendment application and enrichment planting (Tibbett, 2024).

Stabilization-phase sites (10–11 years; R15, R14) migrated toward the forest cluster along PC1 but remained offset along PC2, indicating partial convergence in organic matter and nutrient status while retaining distinct textural and phosphorus signatures. The persistent spatial separation between the stabilization cluster and the forest reference provides quantitative evidence that the system has entered a new equilibrium rather than returning to its original state. This equilibrium, maintained by fundamentally altered mineralogy, depleted iron reserves, and reconstructed rather than natural soil horizons, constitutes what restoration ecologists term a novel ecosystem state. Souza et al. (2025) reached an analogous conclusion in Amazonian bauxite mines, where 9-year natural regeneration plots consistently grouped nearest to reference forests despite considerable intra-site heterogeneity, yet retained measurable separation from the undisturbed reference.

3.8 Toward a novel ecosystem: Implications for adaptive reclamation

Gap analysis across all parameters confirmed that no single soil property achieved complete baseline recovery within the 11-year chronosequence (Table 1, Fig. 9). Soil pH consistently exceeded its reference value and CEC approached parity, yet the three most functionally critical parameters, organic carbon (44.7% mean deficit), total nitrogen (35.0%), and exchangeable iron (80.1%), remained substantially below pre-mining levels. This selective recovery, where acid-neutralizing capacity is restored while biological and micronutrient functions are not, aligns with the five deviated rehabilitation states described by Annandale et al. (2021) in Australian bauxite landscapes and the recovery debt framework proposed by Bizuti et al. (2022). At only 11 years, the system is in the earliest stages of what appears to be a multi-decadal to centennial recovery arc (Nyenda et al., 2021).

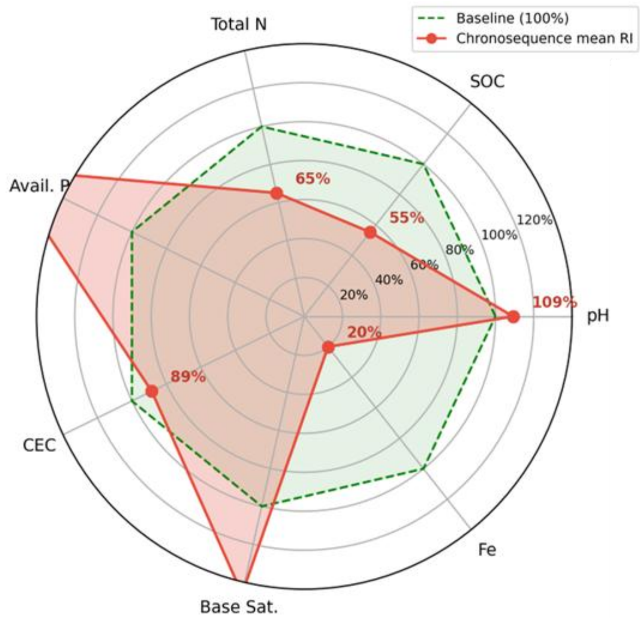

Fig. 9. Gap analysis radar chart showing mean Recovery Index (%) for all parameters across the chronosequence relative to the natural forest baseline (green dashed line = 100%). Red area indicates the extent of recovery deficit

Accepting the trajectory toward a novel ecosystem does not imply abandoning active management. The phase-specific dynamics identified through PCA and cluster analysis indicate that precisely timed interventions can redirect the recovery trajectory toward a more functionally productive endpoint. Three evidence-based recommendations emerge from the integrated analysis (Table 3). First, the transition window at 8–9 years represents the optimal period for intensive organic carbon loading, composted manure at 10–20 Mg ha^{-1} (Larney & Angers, 2012) or combined red mud and cattle manure mixtures (Wanda et al., 2026) because the soil's absorptive capacity and microbial activity are simultaneously accelerating during this phase. Second, iron supplementation through chelated Fe compounds or ferrous sulfate co-applied with organic amendments should target the destabilization phase (5–7 years), when the Fe deficit is most acute and the absence of organic chelating agents most severely restricts phosphorus availability. Third, base cation replenishment through periodic low-dose liming (2–4 Mg ha^{-1}) should extend into the stabilization phase (10+ years) to compensate for the chronic leaching losses documented by declining base saturation trends.

These recommendations align with the broader paradigm shift toward what Xiaochi et al. (2025) term "Technosol construction", the deliberate engineering of soil functional layers through amendment blending, subsoil decompaction, and targeted nutrient delivery. Tibbett (2024) argued that such pedological reconstruction must begin during active mining rather than as a post-closure afterthought, integrating progressive rehabilitation with extraction schedules to minimize topsoil storage duration and preserve seed bank viability. For West Kalimantan specifically, Erusani et al. (2025) called for location-specific amelioration technology that integrates ecological, economic, and social dimensions of post-bauxite sustainability.

The present study carries two limitations not addressed in the Methods. The chronosequence captures only the early-to-intermediate stages of what is likely a centennial-scale process; extending the monitoring window beyond 11 years is essential to determine whether the stabilization-phase equilibrium persists. Microbiological parameters, microbial biomass carbon, enzymatic activity, and community composition were not measured, yet Oneț et al. (2022) and Bateman et al. (2021) have demonstrated that biological indicators often follow trajectories distinct from chemical properties and are essential for holistic rehabilitation assessment. Despite these constraints, the chronosequence data presented here provide the empirical foundation for designing an integrated reclamation framework that acknowledges the inevitability of ecosystem novelty while channeling that novelty toward productive and ecologically resilient land use outcomes.

Table 3. Evidence-based, phase-specific management recommendations derived from chronosequence analysis

Phase	Age (yr)	Constraints	Interventions	Rationale
Destabilization	5-7	Fe collapse (RI 2-13%); SOC <1.2%; P fixation	Chelated Fe + high-dose organic compost (>15 Mg/ha)	Restore Fe-organic complexes; rebuild exchange surfaces
Transition	8-9	SOC deficit (66-72% RI); rapid P flux	Intensive organic loading (10-20 Mg/ha); enrichment planting	Soil absorptive capacity peaks; optimal amendment window
Stabilization	10-11	Chronic base leaching; Fe <40% RI	Periodic liming (2-4 Mg/ha); red mud-organic blends	Prevent regressive acidification; sustained Fe + pH support
Post-stabilization	>11	Novel ecosystem equilibrium; subsoil compaction	Subsoil decompaction; long-term monitoring (>20 yr)	Shift to structural and biological restoration

Note: Recovery phases were delineated by K-means clustering (k = 3) on PCA coordinates, validated by Silhouette analysis. RI = Recovery Index relative to the natural forest baseline

4. Conclusions

Soil chemical recovery across the post-bauxite mining chronosequence at PT XYZ proceeded through three non-linear phases rather than converging monotonically toward the pre-mining forest baseline. The destabilization phase (5–7 years) was characterized by severe depletion of organic carbon, total nitrogen, and exchangeable iron despite above-baseline pH sustained by residual ameliorant alkalinity. The transition phase (8–9 years) marked a period of accelerated biogeochemical flux, during which organic matter accumulation restructured the exchange complex and mobilized previously fixed phosphorus. By the stabilization phase (10–11 years), recovery curves flattened toward a new equilibrium retaining persistent deficits in exchangeable iron (80.1%), organic carbon (44.7%), and total nitrogen (35.0%), indicating that the system is converging toward a novel ecosystem state rather than restoring its pre-mining baseline. Two principal contributions emerge from this study. First, the identification of a critical iron collapse to 2.0% of baseline during the destabilization phase reveals an under-documented micronutrient bottleneck that constrains both iron nutrition and phosphorus availability through the Fe–P antagonism operating at that stage. Second, the PCA-based multivariate analysis provides quantitative evidence that recovery is phase-dependent and directionally distinct from the original forest trajectory — a finding that extends the novel ecosystem framework to the poorly studied post-bauxite landscapes of tropical Southeast Asia.

These findings carry direct implications for reclamation practice. The transition window at 8–9 years represents the optimal period for intensive organic amendments and chelated iron applications, when the soil's absorptive capacity is accelerating, and geochemical conditions are most receptive to nutrient loading. Periodic base cation replenishment through low-dose liming should extend into the stabilization phase to counteract chronic leaching losses documented by declining base saturation trends. Future research should incorporate extended chronosequences beyond 11 years, multi-depth soil sampling, and microbiological indicators to evaluate whether phase-specific interventions may redirect the novel ecosystem trajectory toward sustained functional productivity in tropical post-bauxite landscapes.

Acknowledgement

The author would like to express sincere gratitude to [Faculty of Agricultural Universitas Tanjungpura or Kemendiksainstek] for the financial support provided through the DIPA 2025 funding program. The author also extends appreciation to PT ANTAM Tbk-UBPB West Kalimantan for granting access to the post-bauxite mining sites and providing necessary logistical assistance during the field investigation and soil sampling processes.

Author Contribution

Conceptualization; Methodology; Software; Validation; Formal Analysis; Investigation; Resources; Data Curation; Writing – Original Draft Preparation; Writing – Review & Editing; Visualization; Supervision; Project Administration; and Funding Acquisition. The author has read and agreed to the published version of the manuscript.

Funding

Universitas Tanjungpura funded this research through the DIPA 2025 scheme, grant number 2450/UN22.3/PT.01.03/2025.

Ethical Review Board Statement

Not available.

Informed Consent Statement

Not available.

Data Availability Statement

Not available.

Conflicts of Interest

The author declares no conflict of interest

Declaration of Generative AI Use

During the preparation of this work, the author used Claude AI version Opus 4 (Anthropic, 2025) to assist in refining academic language, formatting data tables, and improving the overall structural clarity of the manuscript. After using this tool, the author reviewed and edited the content as needed and took full responsibility for the content of the publication.

Open Access

References

Annandale, M., Meadows, J., & Erskine, P. (2021). Indigenous forest livelihoods and bauxite mining: A case-study from northern Australia. *Journal of Environmental Management, 294*, 113014. https://doi.org/10.1016/j.jenvman.2021.113014

Bateman, A. M., Erickson, T. E., Merritt, D. J., Veneklaas, E. J., & Muñoz-Rojas, M. (2021). Native plant diversity is a stronger driver for soil quality than inorganic amendments in semi-arid post-mining rehabilitation. *Geoderma*, *394*, 115001. https://doi.org/10.1016/j.geoderma.2021.115001

Bizuti, D. T. G., Robin, A., Soares, T. M., Moreno[1], V. S., Almeida, D. R. A., Andreote, F. D., Casagrande, J. C., Guillemot, J., Herrmann, L., van Melis, J., Perim, J. E. L., de Medeiros, S. D. S., Sorrini, T. B., & Brancalion, P. H. S. (2022). Multifunctional soil recovery during the restoration of Brazil's Atlantic Forest after bauxite mining. *Journal of Applied Ecology*, *59*(9), 2262–2273. https://doi.org/10.1111/1365-2664.14097

Brasil, N. A. B., Schwartz, G., Noronha, N. C., Gama, M. A. P., Ferreira, G. C., Carvalho, E. J. M., & Brasil, N. M. de Q. X. (2025). Seedling planting to restore ecosystems after bauxite mining in Brazilian amazon: The need of monitoring and reviewing techniques and procedures. *Plant Ecology*, *226*(8), 907–920. https://doi.org/10.1007/s11258-025-01539-5

Cavalcante, D. M., Silva, I. R. da, & Oliveira, T. S. de. (2023). Soil quality indicators for monitoring the short-term effects of mined soil rehabilitation strategies for bauxite. *Revista Brasileira de Ciência Do Solo*, *47*, e0220126. https://doi.org/10.36783/18069657rbcs20220126

Charan, K., Banerjee, S., Mandal, J., & Bhattacharyya, P. (2025). Soil stressors on ecophysiology of bauxite mine impacted soil: Heavy metal–acidity–organic matter nexus. *Journal of Environmental Quality*, *54*(2), 435–449. https://doi.org/10.1002/jeq2.20666

Daba, A. (2024). Review on Minerals Transformation and Cycling of Basic Cations in Soil Systems. *SSRN 5167028*. https://papers.ssrn.com/sol3/papers.cfm?abstract_id=5167028

Dibattista, I., Camara, A. R., Molderez, I., Benassai, E. M., & Palozza, F. (2023). Socio-environmental impact of mining activities in Guinea: The case of bauxite extraction in the region of Boké. *Journal of Cleaner Production*, *387*, 135720. https://doi.org/10.1016/j.jclepro.2022.135720

Enescu, C. M., Mircea, M., Ilie, L., Lucian, D., Timofte, A. I., & Gabriel, M. (2025). Afforestation of Degraded Lands: A Global Review of Practices, Species, and Ecological Outcomes. *Forests*, *16*(11), 1743–1775. https://doi.org/10.3390/f16111743

Erusani, A. S., Marimin, M., Suwardi, S., & Hasim, H. (2025). Towards a sustainable future: Managing the post-bauxite mining environmental impact for sustainable development. *IOP Conference Series. Earth and Environmental Science*, *1557*(1), 12021–12034. https://doi.org/10.1088/1755-1315/1557/1/012021

Fernandes, G. W., Lana, T. C., Ribas, C. R., Schoereder, J. H., Solar, R., Majer, J. D., Cordeiro, E. G., Delabie, J. H. C., & Vilela, E. F. (2021). Changes in Epigaeic Ant Assemblage Structure in the Amazon during Successional Processes after Bauxite Mining. *Sociobiology*, *68*(1), e4973–e4973. https://doi.org/10.13102/sociobiology.v68i1.4973

Gao, R., Zhao, B., Wang, J., Shi, W., Wang, H., Zhu, J., Zhang, X., Xia, D., Liu, D., Liu, L., Xia, Z., & Xu, W. (2026). Dynamics of iron-bound organic carbon sequestration in soil-cement aggregates during the ecological restoration process. *Journal of Environmental Chemical Engineering, 14*(1), 120637. https://doi.org/10.1016/j.jece.2025.120637

Ghisman, V., Muresan, A. C., Bogatu, N. L., Herbei, E. E., & Buruiana, D. L. (2025). Recent advances in the remediation of degraded and contaminated soils: A review of sustainable and applied strategies. *Agronomy*, *15*(8), 1920. https://doi.org/10.3390/agronomy15081920

Hartati, W., Amir, M. A., Syahrinudin, S., Syarifudin, A., Sofyan, F. P. M., & Kusuma, F. D. (2025). Soil physical and chemical properties affecting Falcataria falcata diameter in the post-coal mining revegetation. *IOP Conference Series. Earth and Environmental Science*, *1562*(1), 12014–12029. https://doi.org/10.1088/1755-1315/1562/1/012014

Hermansyah, H., Lulu, Y., Eddy, I. and Marsi, M., (2021). Analysis on the characteristics of ex-mining soil after 5 years and 10 years of revegetation. *Media Konservasi, 26*(3), pp.239-247. https://doi.org/10.29244/medkon.26.3.239-247

Larney, F. J., & Angers, D. A. (2012). The role of organic amendments in soil reclamation: A review. *Canadian Journal of Soil Science*, *92*(1), 19–38. https://doi.org/10.4141/cjss2010-064

Lewis, S., & Rosales, J. (2020). Restoration of Forested Lands under Bauxite Mining with Emphasis on Guyana during the First Two Decades of the XXI Century: A Review. *Journal of Geoscience and Environment Protection, 8*, 41-67. https://doi.org/10.4236/gep.2020.811003

Lilay, G. H., Thiébaut, N., du Mee, D., Assunção, A. G. L., Schjoerring, J. K., Husted, S., & Persson, D. P. (2024). Linking the key physiological functions of essential micronutrients to their deficiency symptoms in plants. *New Phytologist, 242*(3), 881–902. https://doi.org/10.1111/nph.19645

Long, Z., Zhu, H., Wu, Y., Ma, Z., Yu, D., & Bing, H. (2024). Aboveground plant biomass drove the reclamation-year dependence of soil quality along a 49-year vegetation reclamation chronosequence. *Plant and Soil*, 1-15. https://doi.org/10.1007/s11104-024-06946-7

Martins, W. B. R., Schwartz, G., Ribeiro, S. S., Ferreira, G. C., de Souza Barbosa, R., de Paula, M. T., Barbosa, V. M., & de Assis Oliveira, F. (2021). Ecosystem restoration after bauxite mining: Favorable indicators for Technosols construction and soil management using liming and subsoiling. *New Forests*, *52*(6), 971–994. https://doi.org/10.1007/s11056-021-09834-5

Nyenda, T., Gwenzi, W., & Jacobs, Sm. (2021). Changes in physicochemical properties on a chronosequence of gold mine tailings. *Geoderma*, *395*, 115037. https://doi.org/10.1016/j.geoderma.2021.115037

Oneț, A., Brejea, R., Dincă, L., Enescu, R., Oneț, C., & Besliu, E. (2022). Evaluation of Biological Characteristics of Soil as Indicator for Sustainable Rehabilitation of a Post-Bauxite-Mining Land. *Diversity*, *14*(12). https://doi.org/10.3390/d14121087

Ouyang, S., Tie, L., Rao, X., Cai, X., Liu, S., Vitali, V., Wei, L., Yu, Q., Sun, D., Lin, Y., Bose, A. K., Gessler, A., & Shen, W. (2023). Mixed-Species Acacia Plantation Decreases Soil Organic Carbon and Total Nitrogen Concentrations but Favors Species Regeneration and Tree Growth over Monoculture: A Thirty-Three-Year Field Experiment in Southern China. *Forests*, *14*(5). https://doi.org/10.3390/f14050968

Prematuri, R., Turjaman, M., Sato, T., & Tawaraya, K. (2020). Post Bauxite Mining Land Soil Characteristics and Its Effects on the Growth of Falcataria moluccana (Miq.) Barneby & J. W. Grimes and Albizia saman (Jacq.) Merr. *Applied and Environmental Soil Science*, *2020*(1), 6764380. https://doi.org/10.1155/2020/6764380

Raj, A., Mandal, J., & Kumari, P. B. (2020). Organo-metallic complex and its implications. *Journal of Pharmacognosy and Phytochemistry*, *9*(2), 491–500. https://doi.org/10.22271/phyto.2020.v9.i2i.10904

Souza, R. S., Noronha, N. C., Brasil, N. A. B., Pereira, W. V. da S., Gama, M. A. P., Senado, J. A. V., Carvalho, E. J. M., Ferreira, G. C., & da Silva Júnior, M. L. (2025). Bauxite mining in the Amazon: Impacts of environmental recovery methods on soil organic matter and physical attributes. *Landscape and Ecological Engineering*, *21*(4), 745–756. https://doi.org/10.1007/s11355-025-00669-2

Spletozer, A. G., Fernandes Filho, E. I., Martini, A., Bramorski, J., Tonello, K. C., & Dias, H. C. T. (2024). Surface runoff in six years of rehabilitation of two areas after bauxite mining in Southeastern Brazil. *Ecological Engineering*, *202*, 107231. https://doi.org/10.1016/j.ecoleng.2024.107231

Sulakhudin, Sukirno, & Abdilla, A. M. (2023). Impact of Bauxite Mining on Soil Chemical Properties at Several Depths. *IOP Conference Series: Earth and Environmental Science, 1165*(1), 012024. https://doi.org/10.1088/1755-1315/1165/1/012024

Sulakhudin, Herawatiningsih, R., Krisnohadi, A., Abdillah, A. M., Santi, & Mudim. (2024a). Impact of red mud on soil properties and revegetation species growth in bauxite mining land reclamation. *Journal of Degraded and Mining Lands Management, 12*(1), 6509–6518. https://doi.org/10.15243/jdmlm.2024.121.6509

Sulakhudin, Sukirno, & Abdillah, A. M. (2024b). Monitoring soil fertility to mitigate soil degradation in reclamation land after bauxite mining. *IOP Conference Series: Earth and Environmental Science*, *1314*(1), 012011. https://iopscience.iop.org/article/10.1088/1755-1315/1314/1/012011/meta

Suswati, D., & Denashurya, N. I. (2023). Sustainable Rehabilitation of Post-Bauxite Mining Land for Albizia falcata Cultivation Using Specific Location Amelioration Technology. *Sustainability*, *15*(14). https://doi.org/10.3390/su151410959

Tang, Y., Zhao, Y., Li, Z., Meichen, H., Sun, Y., Hong, Z., & He, R. (2025). A Comprehensive Evaluation of Land Reclamation Effectiveness in Mining Areas: An Integrated Assessment of Soil, Vegetation, and Ecological Conditions. *Remote Sensing*, *17*(10), 1744. https://doi.org/10.3390/rs17101744

Tibbett, M. (2024). Post-mining ecosystem reconstruction. *Current Biology*, *34*(9), R387–R393. https://doi.org/10.1016/j.cub.2024.03.065

Tsapko, Y., Kucher, A., Meshref, B., Krupin, V., Rozmarina, A., Holovina, O., & Skorokhod, I. (2023). Structural Amelioration of Soils for Sustainable Land Management. *Land, 12*(4). https://doi.org/10.3390/land12040909

Wanda, W., Akbar, A. A., Putri, E. A. W., & Suhartoyo, A. (2026). Rehabilitation of disturbed land in bauxite mining: Challenges and prospects in Sanggau, West Kalimantan, Indonesia. *Journal of Degraded and Mining Lands Management, 13*(1), 9259–9269. https://doi.org/10.15243/jdmlm.2026.131.9259

Wu, S., Liu, Y., Southam, G., Robertson, L. M., Wykes, J., Yi, Q., Hall, M., Li, Z., Sun, Q., Saha, N., Chan, T.-S., Lu, Y.-R., & Huang, L. (2021). Rhizosphere Drives Biotite-Like Mineral Weathering and Secondary Fe–Si Mineral Formation in Fe Ore Tailings. *ACS Earth and Space Chemistry*, *5*(3), 618–631. https://doi.org/10.1021/acsearthspacechem.0c00331

Xie, X., Zhu, B., Yan, X., Zhng, G., & Huang, J. (2025). Titanium white waste acid-mediated dealkalization and doil-Like substrate construction from Bauxite Residue: Mechanisms and ecological benefits. *Journal of Environmental Sciences*. https://doi.org/10.1016/j.jes.2025.12.012

Xiaochi, M., Wang, W., Han, F., Binxian, J., Liu, Y., Yuhui, G., Ma, Y., Jinggui, W., & Wu, S. (2025). Technosol Construction for Sustainable Agriculture: Research Status and Prospects. *Agronomy*, *15*(12), 2903–2925. https://doi.org/10.3390/agronomy15122903

Yadav, S. K., Banerjee, A., Jhariya, M. K., Meena, R. S., Khan, N., & Raj, A. (2022). Eco-restoration of bauxite mining: An ecological approach. In *Natural resources conservation and advances for sustainability* (pp. 173-193). Elsevier. https://doi.org/10.1016/B978-0-12-822976-7.00028-4

Yang, X., Liu, C., Liang, C., Wang, T., & Tian, J. (2024). The Phosphorus-Iron Nexus: Decoding the Nutrients Interaction in Soil and Plant. *International Journal of Molecular Sciences*, *25*(13). https://doi.org/10.3390/ijms25136992

Biographies of Author

Sulakhudin, Department Soil Science, Faculty of Agriculture, Universitas Tanjungpura, Pontianak, West Kalimantan, 78124, Indonesia.

- Email: sulakhudin@faperta.untan.ac.id
- ORCID: 0000-0002-8593-9206
- Web of Science ResearcherID: AGU-2240-2022
- Scopus Author ID: 56888768200
- Homepage: https://scholar.google.co.id/citations?user=tnzdAugAAAAJ&hl=id